ACS APPLIED MATERIALS & INTERFACES

Research Article

www.acsami.org

# Electron Transfer Mediated Electrochemical Biosensor for MicroRNAs Detection Based on Metal Ion Functionalized Titanium Phosphate Nanospheres at Attomole Level

Fang-Fang Cheng,[†] Ting-Ting He,[†,‡] Hai-Tiao Miao,[†] Jian-Jun Shi,[†,‡] Li-Ping Jiang,*[,†] and Jun-Jie Zhu*[,†]

[†]State Key Lab of Analytical Chemistry for Life Science, School of Chemistry and Chemical Engineering, Nanjing University, Nanjing 210093, P. R. China

[‡]School of Chemical Engineering, Anhui University of Science and Technology, Huainan 232001, China

Supporting Information

**ABSTRACT:** MicroRNAs (miRNAs) have emerged as new candidates as diagnostic and prognostic biomarkers for the detection of a wide variety of cancers; thus, sensitive and selective detection of microRNAs is significant for early-phase cancer diagnosis and disease prevention. A novel and simple electrochemical miRNA biosensor was developed using $Cd^{2+}$-modified titanium phosphate nanoparticles as signal unit, two DNA as capture probes, and $Ru(NH_3)_6^{3+}$ as electron transfer mediator. Large quantities of cadmium ions were mounted in titanium phosphate spheres to output the electrochemical signal. Because of the presence of $Ru(NH_3)_6^{3+}$ molecules that interacted with DNA base-pairs as electron wire, the electrochemical signal significantly increased more than 5 times. This approach achieved a wide dynamic linear range from 1.0 aM to 10.0 pM with an ultralow limit detection of 0.76 aM, exerting a substantial enhancement in sensitivity. Moreover, the proposed biosensor was sufficiently selective to discriminate the target miRNAs from homologous miRNAs and could be used for rapid and direct analysis of miRNAs in human serum. Therefore, this strategy provides a new and ultrasensitive platform for miRNA expression profiling in biomedical research and clinical diagnosis.

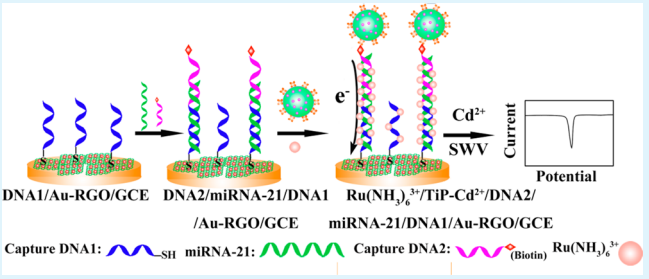


**KEYWORDS:** *microRNAs, titanium phosphate, electron transfer, electrochemical biosensor*

## INTRODUCTION

miRNAs are a class of nonprotein-coding small RNA molecules with 17−25 nucleotides that regulate multiple genes associated with human cancers, neurological diseases, and viral infections via binding to corresponding messenger RNAs (mRNAs) to induce the mRNA degradation or translation blocking.[1] Distinct miRNA expression patterns are associated with various tumor types. miRNA-155, miRNA-21, miRNA-205, miRNA-17-92, etc. have been found overexpressed in many cancer types including hematopoietic cancers and breast, lung, and colon cancers.[2−4] Therefore, miRNAs have been potential biomarkers that could serve for early disease diagnosis as well as for assessing the prognosis and monitoring the response to the treatment.

For the quantification of miRNAs, their small size, high sequence similarity, and low expression levels impose great challenges in the analysis using conventional techniques including Northern blotting,[5,6] quantitative reverse-transcriptase polymerase chain reaction (qRT-PCR),[7,8] and microarrays.[9,10] Numerous new strategies such as colorimetric measurement,[11−13] fluorescence detection,[14,15] electrochemical detection,[16−18] surface plasmon resonance,[19] bioluminescence technology,[4] chemiluminescence technology,[20] electrochemiluminescence methods,[21] and capillary electrophoresis assays[22] have been developed to improve the detection sensitivity and flexibility. Among these methods, electrochemical (EC) biosensors have attracted increasing attention because of their low cost, convenient operation, rapid detection, and good sensitivity.[23] EC methods usually involved either label-free or miRNA labeling.[24] Schiavo and co-workers published a label-free method based on G oxidation signal of G-rich miRNAs after hybridization with a G-free probe at carbon electrodes.[25] However, the use of a G-free probe limited the application in the detection of G-free miRNAs, and meanwhile it showed a lower sensitivity. To overcome these difficulties, labeling methods integrated with signal amplification strategies such as nanoparticles-based amplification,[26,27] enzymatic signal amplification,[28] and rolling circle amplification[29,30] have been developed. With the development of nanotechnology, a variety of nanoparticles including quantum dots,[31] gold nanoparticles,[32−34] and oxidase-like nanoparticles[27,35,36] are widely used in the fabrication of the biosensor as signal sources. Wang et al. developed a miRNA biosensor by combining rolling circle amplification (RCA), quantum dots tagging, and anodic

Received: December 11, 2014
Accepted: January 14, 2015
Published: January 14, 2015





DOI: 10.1021/am508690x
ACS Appl. Mater. Interfaces 2015, 7, 2979−2985

stripping voltammetric detection (ASV).[37] The method could specifically quantify miRNA-16 over a 6-decade dynamic range and reach an ultralow detection limit of 0.32 aM. However, in the control rolling circle amplification process, it may be complicated and difficult. Furthermore, quantum dots need to be dissolved in acid solution before electrochemical detection. Our group previously provided a novel multianalyte electrochemical immunoassay for ultrasensitive detection of human cardiopathy biomarkers cardiac troponin I (cTnI) and human heart-type fatty-acid-binding protein (FABP) by using metal ion functionalized titanium phosphate nanospheres (TiP) as labels.[38] The proposed immunoassay exhibited high sensitivity and selectivity for the detection. Most importantly, the TiP−$Cd^{2+}$ conjugates could be detected directly without acid dissolution, which would greatly simplify the detection steps. Therefore, TiP−$Cd^{2+}$ conjugates are potential labels for the electrochemical detection of miRNAs.

MiRNA detection is often performed using sandwich assays via nucleotide hybridization because it is difficult to label miRNAs directly in a biological matrix.[25] DNA-based genosensor is usually related to the electrical conductivity of DNA. At present, it is generally recognized that a $\pi$-stacked double-stranded (ds) DNA molecule is an efficient one-dimensional electrical conductor[39] and that the capability of transporting electrons is comparable to that of conventional conducting polymers[40,41] and only 100 times less efficiently than a metal wire.[42] However, in fact, arguments on the mechanisms of electron transfer (ET) properties of dsDNA still exist, and the electron transfer efficiency of DNA over long distances is not completely clear.[43−45] Abi and Ferapontova reported that the ET communication between the electrode and anthraquinone, built in DNA through the acetylene linker, was achieved only when $Ru(NH_3)_6^{3+}$ molecules were electrostatically attached to the DNA duplex to form the electronic wire.[46]

Herein, an ultrasensitive electrochemical genosensor based on two DNAs as the target capturers and $Cd^{2+}$ functionalized titanium phosphate nanosphere (TiP−$Cd^{2+}$) as a label is fabricated for the detection of miRNA-21. Large amounts of $Cd^{2+}$ ions were incorporated into the TiP nanospheres, providing high electrochemical signals. $Ru(NH_3)_6^{3+}$ molecules are introduced to interact with DNA base-pairs as an "electron bridge" for electron transport. The results indicated that $Ru(NH_3)_6^{3+}$ greatly improved the electron transfer and significantly enhanced signals. Therefore, the proposed biosensor exhibited good sensitivity and selectivity with a low detection limit of 0.76 aM and could meet the requirements for direct detection of miRNA-21 in human serum, showing its great potential for cancer diagnosis.

## EXPERIMENTAL SECTION

**Materials and Reagents.** Streptavidin protein (SA) was purchased from Beijing Biosynthesis Biotechnology Co., Ltd. (Beijing, China). Graphite powder (KS-10), bovine serum albumin (BSA), 1-ethyl-3-(3-(dimethylamino)propyl)carbodiimide hydrochloride (EDC), *N*-hydroxysuccinimide (NHS), poly(allylamine hydrochloride) (PAH), 6-mercapto-1-hexanol (MCH), chloroauric acid ($HAuCl_4$), hexaamine ruthenium(III) chloride ($Ru(NH_3)_6Cl_3$), and Tween-20 were from Sigma-Aldrich. Glutaraldehyde (GLU) was obtained from Shanghai Reagent Company (Shanghai, China). Tetrabutyl titanate (TBOT), docusate sodium salt (AOT), and $H_3PO_4$ were from Nanjing Chemical Reagent Co., Ltd. (Nanjing, China). Agarose and diethyl pyrocarbonate (DEPC) were purchased from Beyotime Institute of Biotechnology (Nantong, China). DNA oligonucleotides were purchased from Shanghai Sangon Biological Engineering Technology & Services Co. (China). miRNA-21 oligonucleotides were obtained from Shanghai Genepharma Co., Ltd. (Shanghai, China) (Table 1). Phosphate-buffered saline (PBS)

**Table 1. Oligonucleotide Sequences Employed in the Present Work**

| | sequences (5′→3′)[a] |
|---|---|
| miRNA-21 | UAGCUUAUCAGACUGAUGUUGA |
| capture DNA1 | SH-C3-TCAACATCAGT |
| capture DNA2 | $PO_4$−CTGATAAGCTA-Biotin |
| 1-base mismatch | UAACUUAUCAGACUGAUGUUGA |
| 3-bases mismatch | UAACUUAUCACACUGAUGUCGA |

[a]The underlined letters refer to the mismatched bases.

solutions with different pH values were prepared by mixing the stock solution of $NaH_2PO_4$ and $Na_2HPO_4$ and then adjusting the pH with 0.1 M NaOH and $H_3PO_4$. HAc/NaAc solutions with different pH values were prepared by mixing the stock solutions of HAc and NaAc. Human serum is from Gulou Hospital (Nanjing, China). All other reagents were of analytical reagent grade and used without further purification. All aqueous solutions were prepared using DEPC-treated ultrapure water from a Milli-Q system (Millipore, Billerica, MA, U.S.A.).

**Apparatus.** All electrochemical measurements were performed on a CHI 660D workstation (Chenhua, Shanghai, China) with a conventional three-electrode system composed of a platinum wire as the auxiliary, a saturated calomel electrode as the reference, and the modified glass carbon electrode (GCE) as the working electrode. Transmission electron micrographs (TEM) were measured on a JEOL JEM 200CX transmission electron microscope using an accelerating voltage of 200 kV. Electrochemical impedance spectroscopy (EIS) was performed with an Autolab electrochemical analyzer (Eco Chemie, The Netherlands) in a 10 mM $K_3Fe(CN)_6/K_4Fe(CN)_6$ (1:1) mixture with 1.0 M KCl as the supporting electrolyte, using an alternating current voltage of 5.0 mV, within the frequency range of 0.01 Hz−100 kHz.

**Preparation of Strepavdin−TiP−Metal Ion Probes.** First, TiP nanospheres were synthesized according to the literature.[38,47] Briefly, 5 g of AOT was dissolved into 32 mL of ethanol, and $H_3PO_4$ (6 mL) was added to get a turbid solution. Then, a mixture of TBOT with ethanol (1.75 g/32 mL) was dropped quickly into the AOT/ethanol solution and ultrasonically mixed to get a stable mixture solution. The mixture was stirred at 80 °C for 6 h. The solid product was washed with ethanol and deionized (DI) water for several times to remove the residual phosphoric acid and surfactant. For ion exchange, 1 mL of TiP nanospheres (40 mg $mL^{-1}$) was dispersed into 30 mL of 10 mM $Cd(NO_3)_2$ aqueous solution and stirred at 50 °C for 24 h. The resulting hybrid nanospheres were obtained by centrifugation and rinsed with water several times. The TiP−$Cd^{2+}$ products were dispersed into 2 mL of DI water with the concentration of 20 mg $mL^{-1}$. Next, 2 mL of the TiP−$Cd^{2+}$ hybrids were dispersed into 2 mL of PAH (2 mg $mL^{-1}$) aqueous solution and sonicated for 20 min. Then, the hybrids were washed with DI water, dispersed into 2 mL of GLU (0.25 wt %), and sonicated for 5 min. After washing with DI and PBS three times, 600 $\mu$L of SA (0.01 mg $mL^{-1}$) solution was added into the TiP−$Cd^{2+}$ hybrids and shaken for 6 h. After centrifugation, the obtained bioconjugates were further washed with PBS at least three times and resuspended in 8 mL of tris buffer (pH = 7.4) as the assay solution.

**Sensor Fabrication.** Graphene oxide (GO) was prepared by a modified Hummers method using graphite powder as the starting material.[48] Polyethylenimine (PEI)-modified graphene/Au composites (Au-RGO) were prepared by the following procedure. In brief, the mixture containing GO (10 mL, 0.05 mg $mL^{-1}$) and PEI (10 mL, 2 mg $mL^{-1}$) was sonicated for 30 min and reacted at 90 °C for 6 h in the round-bottomed flask. The as-prepared PEI-grafted graphene (RGO) was centrifuged at 22 000 rpm for 30 min, washed several times with


DOI: 10.1021/am508690x
ACS Appl. Mater. Interfaces 2015, 7, 2979−2985

deionized water, and redispersed in water with a final concentration of 1.0 mg $mL^{-1}$ for further use. Colloidal Au nanoparticles (NPs) with an average diameter of ~10 nm were prepared as reported previously.[49] Then the RGO dispersion was added into AuNPs solution (the volume ratios of RGO/Au = 1:3) and sonicated for 30 min to obtain PEI-modified graphene/Au composites (Au-RGO). Au-RGO composites were further washed with water three times and redispersed in water at a concentration of 1 mg $mL^{-1}$ for further use. The glass carbon electrode (GCE) with a diameter of 3 mm was polished using 0.3 and 0.05 $\mu$m alumina slurry followed by rinsing thoroughly with water. After successive sonication in 1:1 nitric acid, acetone, and water, the GCE was dried with nitrogen. Ten $\mu$L of Au-RGO composite solution was dropped on the fresh pretreated GCE and allowed to dry at room temperature to obtained Au-RGO-modified GCE (Au-RGO/GCE).

Thiol-capturer DNA1 (probe 1, 5 $\mu$L, 10 $\mu$M) was activated with tris(2-carboxyethyl)phosphine (TCEP) (5 $\mu$L, 10 mM) for 0.5 h to prevent the terminal cysteine from forming disulfide bonds and then mixed with 10 $\mu$L of tris buffer solution (TBS, pH = 7.4, 10 mM). The mixture was dropped on the Au-RGO/GCE electrode and reacted at 4 °C for 16 h in humidified surroundings. Finally, the electrode was washed with TBS several times, immersed into 10 $\mu$L of 1 mM MCH for 1 h at room temperature to block the nonspecific binding sites, and then washed with TBS.

**RNA Hybridization Assay and Measurement Procedure.** To carry out the RNA hybridization assay, the modified electrode was first incubated with a 12 $\mu$L drop containing the target RNA (miRNA-21 with different concentrations or serum samples, 5 $\mu$L), capturer DNA2 (probe 2, 5 $\mu$L, 10 $\mu$M), T4 DNA ligase (1 $\mu$L, 1000 U $\mu L^{-1}$), and 10× TBS (1 $\mu$L, 100 mM) for 4 h at 37 °C to perform the hybridization reaction, followed by washing with TBS three times. Next, it was further incubated with 10 $\mu$L of TiP−$Cd^{2+}$−SA bioconjugate solution for 60 min at 37 °C and then washed thoroughly with TBS (containing 1% BSA) to remove nonspecifically bound conjugates. $Ru(NH_3)_6^{3+}$ (10 $\mu$L, 1 mM) was dropped on the electrode and followed by washing with TBS three times. After treatment with $Ru(NH_3)_6^{3+}$, the electrochemical measurement was carried out in 3 mL of HAc/NaAc (pH 4.6, 0.2 mol $L^{-1}$) containing $Bi^{3+}$ ion at a final concentration of 10 $\mu$g $mL^{-1}$.[50] The analytical procedure involved an electrodeposition at −1.2 V for 120 s and square wave voltammetry (SWV) scanning from −1.0 to −0.4 V with a pulse amplitude of 25 mV, a pulse frequency of 15 Hz, and a quiet time of 2 s.[51] The electrochemical responses were recorded at about −0.68 V for quantitative measurement of miRNA-21.

**Polyacrylamide Gel Electrophoresis Analysis.** Polyacrylamide gel (8%) was employed to verify the binding of miRNA-21 with DNA1 and DNA2. First, 2 $\mu$L of 10 $\mu$M DNA1 and 2 $\mu$L of 10 $\mu$M DNA2 were incubated with 2 $\mu$L of 10 $\mu$M miRNA-21 in Tris-HCl buffer (pH = 7.4, 10 mM) at 37 °C for 4 h to form stable DNA hybrid by a base-pairing hybridization. Electrophoresis was carried out at 100 V for 45 min at room temperature. After separation, the gel was stained with ethidium bromide (EB) and imaged by a Bio-Rad imaging system (Hercules, CA, U.S.A.).

## RESULTS AND DISCUSSION

**Characterization of TiP−$Cd^{2+}$/SA.** TiP nanoparticles with uniform morphology, size distribution, and good dispersion were synthesized. As shown in Figure 1A, PAH was modified on TiP−$Cd^{2+}$ via the covalent reaction between the phosphate group of TiP−$Cd^{2+}$ and the amine group of PAH. Then SA was attached to TiP−$Cd^{2+}$ using the glutaraldehyde as a cross-linking agent. The average diameter of TiP was ~100 nm (Figure 1B). After ions changing with $Cd^{2+}$, no size difference was observed between TiP and TiP−$Cd^{2+}$ (Figure 1C). As shown in Figure 1D, SA layers could be observed on the surface of TiP−$Cd^{2+}$, indicating the successful decoration of SA. Furthermore, the reaction concentration of SA was investigated. As shown in Figure S1, Supporting Information, with the

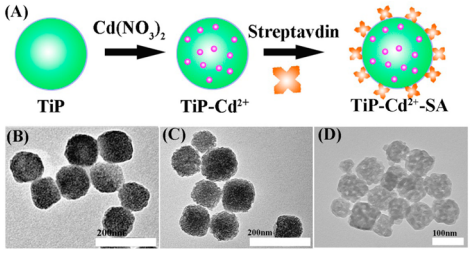


**Figure 1.** (A) Preparation procedures of SA-functionalized TiP−$Cd^{2+}$. TEM images of TiP (B), TiP−$Cd^{2+}$ (C), and TiP−$Cd^{2+}$−SA (D).

increase of SA concentration, the coating amount of SA increased. But when the concentration of SA increased to 0.1 mg $mL^{-1}$, TiP−$Cd^{2+}$−SA aggregated. Thus, the concentration of SA at 0.01 mg $mL^{-1}$ is chosen in the following experiments.

**Principle of the Sensor.** The principle of the TiP−$Cd^{2+}$ probes for electrochemical miRNA biosensing is outlined in Scheme 1. Gold nanoparticle modified graphene (Au-RGO) is

**Scheme 1. Schematic Illustration of the Stepwise Sensor Construction Process**

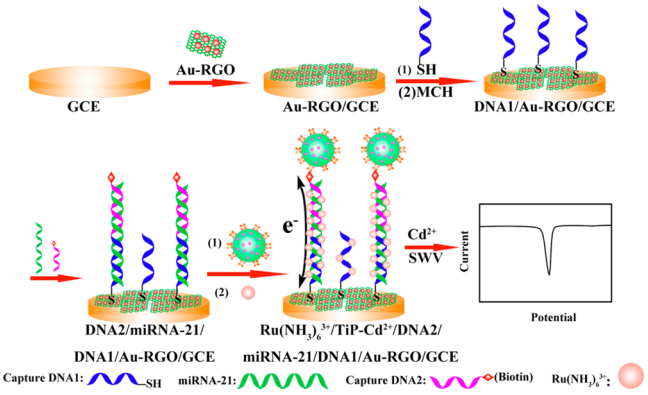


immobilized on a glass carbon electrode (GCE) surface. Thiol-DNA1 is attached to Au-RGO via Au−S bonds. DNA1 and DNA2 both own 11 bases that are complementary to the half part of miRNA-21, respectively. Only in the presence of target miRNA (miRNA-21) and biotin-labeled reporter DNA2 can the sandwich structure form. Then, strepavidin-modified TiP−$Cd^{2+}$ (TiP−$Cd^{2+}$−SA) is further attached to DNA2 via biotin−avidin conjugation as signal tags. Finally, $Ru(NH_3)_6^{3+}$ molecules are incorporated into the duplex DNA via the electrostatic interaction to accelerate the electron transfer. The corresponding electrochemical current responses of $Cd^{2+}$ are used to quantify the concentration of miRNA-21.

**Characterization of the Genosensor.** To facilitate the immobilization of the capture DNA1, gold nanoparticle (AuNP)-functionalized PEI-modified graphene nanosheet (Au-RGO) hybrids with good conductivity and biocompatibility were fabricated via a simple sonication-induced assembly and used as biosensor platforms. The obtained Au-RGO hybrid architecture was confirmed by the TEM image as shown in Figure 2A. AuNPs of 10 nm were distributed homogeneously on the graphene sheet surface. EIS was an effective and sensitive method to characterize the conductivity of the electrode surface. The semicircle diameter at higher frequencies is related to the electron-transfer resistance (Ret), and the linear part at lower frequencies corresponds to the diffusion process. The stepwise construction process of the microRNA


DOI: 10.1021/am508690x
ACS Appl. Mater. Interfaces 2015, 7, 2979−2985

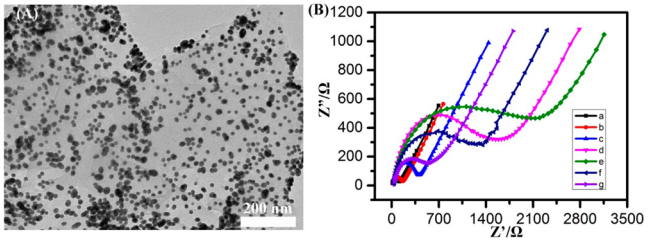


**Figure 2.** (A) TEM image of Au-RGO; (B) Nyquist diagram of electrochemical impedance spectra recorded from 0.01 to $10^5$ Hz for $[Fe(CN)_6]^{3-/4-}$ (10 mM, 1:1) in 1.0 M KCl using a bare GCE (a), Au-RGO/GCE (b), and DNA1/Au-RGO/GCE without (c) or with the modification of MCH (d), DNA2/miRNA-21/DNA1/Au-RGO/GCE (e), and the TiP−$Cd^{2+}$−SA/DNA2/miRNA-21/DNA1/Au-RGO/GCE in the absence (f) or in the presence of $Ru(NH_3)_6^{3+}$ (g).

biosensor was characterized by EIS as shown in Figure 2B. The bare GCE (curve a) and Au-RGO-modified GCE (Au-RGO/GCE, curve b) exhibit nearly straight lines, reflecting excellent conductivity. When DNA1 was loaded on the surface of Au-RGO/GCE, the Ret increased (curve c) to 180 Ω, which suggested that DNA1 formed an additional barrier and further prevented the redox probe to the electrode surface due to the electrostatic repulsion between negative charges of the DNA1 phosphate backbone and the $[Fe(CN)_6]^{3-/4-}$ ions, as well as demonstrated that DNA1 had been successfully immobilized on the electrode. After nonconductive MCH was used to block nonspecific sites and DNA1 hybridized with miRNA-21 and DNA2, larger semicircles (curve d is ∼700 Ω and curve e is 1047 Ω) were observed due to the insulating properties of MCH and the increased negative charges of the nucleotide. However, when TiP−$Cd^{2+}$−SA and $Ru(NH_3)_6^{3+}$ were attached onto the electrode surface, the Ret significantly decreased to 620 Ω (curve f) and 292 Ω (curve g), respectively, which might be attributed to the introduction of positively charged metal ions that improved the electrostatic interaction with $[Fe(CN)_6]^{3-/4-}$, and meanwhile $Ru(NH_3)_6^{3+}$ accelerated electron transfer as a conductor wire. These results indicated that the biosensor was effectively and successfully fabricated.

The hybridization reaction between the target and the capture probes was further analyzed by polyacrylamide gel electrophoresis. In Figure S2, Supporting Information, the first four lanes showed the marker, DNA1, DNA2, and miRNA-21, respectively. No bands were observed in lanes 2 and 3, because DNA1 and DNA2 are single-stranded sequences, while EB usually stains DNA duplex via its intercalation with the stacked base pairs. Lane 4 displayed a band for miRNA-21. In lane 5, another band appeared between 20 and 25 bp compared with lane 4, indicating the formation of DNA1/miRNA-21 complex. In lane 6, the band is brighter than that in lanes 3 and 4, demonstrating the formation of DNA2/miRNA-21 complex. The band in lane 7 has no significant difference comparing to lane 5. However, in the presence of T4 DNA ligase (lane 8), a wide band appeared at the position of >200 bp because T4 DNA ligase is a polypeptide so that DNA1/miRNA-21/DNA2/T4 complex exhibited a relatively low mobility, indicating the successful formation of DNA1/miRNA-21/DNA2/T4 complex.

**Optimization of Conditions.** The comparison of the performances of the assay with or without $Ru(NH_3)_6^{3+}$ is shown in Figure 3A. As we predicted, in the presence of $Ru(NH_3)_6^{3+}$, the peak current is ∼5 times higher than that in the absence of $Ru(NH_3)_6^{3+}$, indicating that $Ru(NH_3)_6^{3+}$ molecules were electrostatically attracted to the DNA duplex; as a result, the electronic wire mediated ET between the electrode and TiP−$Cd^{2+}$ formed, leading to great enhancement of electron transfer. For RNA hybridization, hybridization time is an important parameter. In Figure 3B, the current increased along with the increase of hybridization time from 1 to 4 h, but leveled off at longer time. Moreover, the dependence of the SWV peak current under different pH values of the detection solution was investigated (Figure 3C). The highest electrochemical signal was obtained at a pH of 4.6. Therefore, the incubation time of 4 h was selected as the optimal reaction time and 0.2 M HAc/NaAc (pH 4.6) was selected as the electrolyte for the electrochemical assay in all subsequent work.

**Electrochemical Detection of Target miRNA.** Under optimal conditions, a series of different concentrations of miRNA-21 were measured to confirm the ability of the designed electrochemical biosensor to detect microRNAs. As shown in Figure 4A, the electrochemical signal increased with

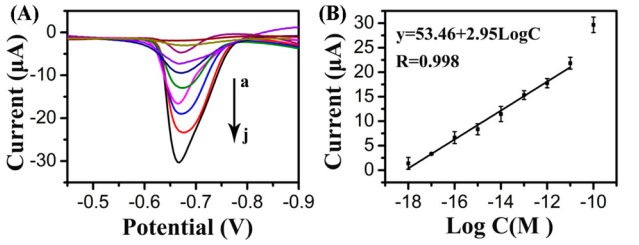


**Figure 4.** (A) SWV of the sensor recorded on Au-RGO/GCE with increasing miRNA-21 concentration from (a) to (j): 0, $10^{-18}$, $10^{-17}$, $10^{-16}$, $10^{-15}$, $10^{-14}$, $10^{-13}$, $10^{-12}$, $10^{-11}$, and $10^{-10}$ M. (B) The linear relationship between the peak current and the logarithm of the target miRNA-21 concentration from $10^{-10}$ M to $10^{-18}$ M. Each value is the average of six measurements.

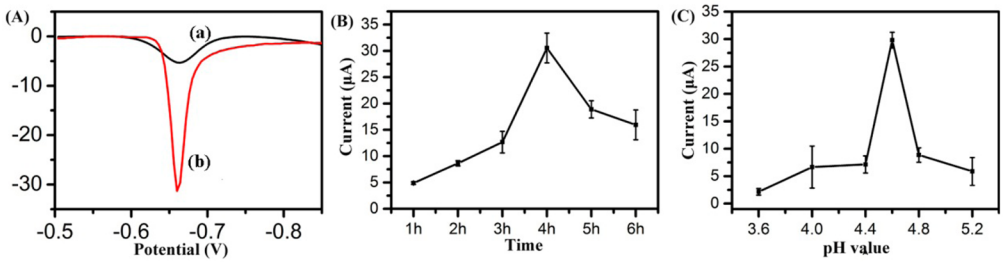


**Figure 3.** (A) Effects of the absence (a) or presence (b) of $Ru(NH_3)_6^{3+}$, (B) hybridization time, and (C) pH value of buffer solution in the RNA sensor. The miRNA-21 concentration is $10^{-10}$ M.


DOI: 10.1021/am508690x
ACS Appl. Mater. Interfaces 2015, 7, 2979−2985

**Table 2. Detection Limits of Various Methods for miRNA Detection**

| method | analyte | LOD | linear range | readout | ref |
|---|---|---|---|---|---|
| cross-catalyst strand-displacement network (CC-SDR) | let-7a | 0.68 fM | 1.0 fM to 10.0 fM | chemiluminescence | 20 |
| exponential amplification reaction (EXPAR) | let-7a | 0.1 zmol | 0.1 zmol to 1.0 fmol and 1.0 fmol to 1.0 pmol | fluorescence | 53 |
| cascade RCA-NESA-DNAzyme amplification | let-7d | 2.0 aM | 100 fM to 1 fM | colorimetry | 11 |
| horseradish peroxidase catalysis | let-7c | 2.0 fM | 5.0 fM to 2.0 pM | electrochemistry | 18 |
| RCA and quantum dots amplification | miRNA-16 | 0.32 aM | 10.0 aM to 10.0 pM | electrochemistry | 37 |
| amplified voltammetric detection by Fc-capped gold nanoparticle amplification | miRNA-182 | 10.0 fM | 10 fM to 2.0 pM | electrochemistry | 34 |
| p19 protein binding and displacement methods | miRNA-32 | 5.0 aM | 10 aM to 1 $\mu$M | electrochemistry | 17 |
| triple signal amplification of multifunctional gold nanoparticles, enzymes, and redox-cycling reaction | miRNA-21 | 3.0 fM | 10 fM to 5 pM | electrochemistry | 54 |
| electron transfer mediated and nanoparticles-tagged amplification | miRNA-21 | 0.76 aM | 1.0 aM to 10.0 pM | electrochemistry | present work |

the increasing concentration of target used for hybridization and showed a good linear correlation versus the logarithm of target miRNA concentrations in the range from 1.0 aM to 10.0 pM (Figure 4B) with the limit of detection (LOD) of 0.76 aM, corresponding to 3.8 ymol of target in 5 $\mu$L of sample solution. The regression equation is $I = 2.95 \log C_{\text{miRNA-21}} + 53.46$ with a correlation coefficient of 0.998, where $I$ and $C$ represent the current intensity and the miRNA-21 concentration, respectively. The typical levels of circulating microRNAs in serum are from 200 aM to 20 pM,[52] which is a subset of the detection range of our proposed method. The limit of detection was estimated from three times the current value of the blank sample detection (free of target miRNA). The low detection limit was attributed to the signal amplification enabled with $Cd^{2+}$-functionalized TiP nanospheres and $Ru(NH_3)_6^{3+}$. Table 2 summarizes the detection limits of some recent reported signal amplification nucleic acids assays. This comparison clearly highlighted the remarkable enhanced LOD of electrochemical biosensor strategy. Although the detection limit of the electrochemical biosensor is not the lowest, the procedure is simpler via sandwich assays than other methods such as fluorescence, chemiluminescence, and colorimetry. Moreover, the linear range is widest with 8 orders of magnitude via electrochemical detection, which is a benefit for future practical application in biomedical fields.

**Specificity.** Sequence specificity in miRNAs detection is an important consideration because miRNA families often possess closely homologous sequences. The specificity of the miRNA biosensor was investigated through a comparison assay on mismatch targets and perfect complementary target, including complementary target, single-base mismatched strand, and three-base mismatched strand at a same concentration of 100 pM. As Figure 5A illustrates, the current of a perfectly complementary target was 10.6 times higher than the single-base mismatch sequence, and the response of the three-base mismatch strand was almost ignored. These results suggested that the sensor owned high sequence specificity and excellent discrimination for similar miRNAs.

**MicroRNA Detection in Serum Samples.** miRNA-21 is overexpressed in a wide variety of cancers. Therefore, the direct detection of the expression level of miRNA-21 in the human blood serum extracted from patients was explored to validate the practicality of this method. miRNA-21 in the human blood serum from three types of cancer patients, including cervical cancer, breast cancer, and leukemia patients, was measured.

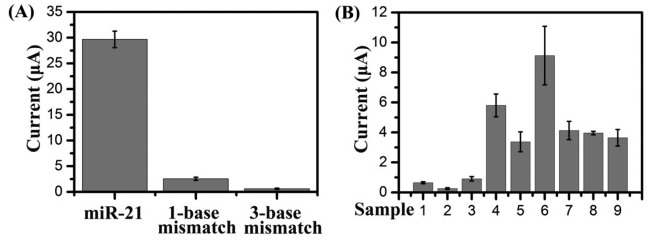


**Figure 5.** (A) SWV signals in the presence of miRNA-21, 1-base mismatch miRNA, and 3-base mismatch miRNA (all at a concentration of $10^{-10}$ M). Each value is the average of three measurements. (B) SWV signals of miRNA-21 in human blood serum obtained by electrochemical biosensor. Samples 1−3 are from three healthy persons. Samples 4 and 5 are from two cervical cancer patients. Samples 6 and 7 are from two breast cancer patients. Samples 8 and 9 are from two leukemia patients. Each value is the average of six measurements.

The electrochemical signal of miRNA-21 in cancer patients is significantly higher (>5 times) than that in the healthy group as shown in Figure 5B, suggesting an upregulation of miRNA-21 in cancer patient human blood serum.[55,56] The miRNA-21 concentration in sample 6 (breast cancer patient, $\sim 9.2 \times 10^{-16}$ M, which is consistent with the previous report[57]) is even 900-fold compared with sample 2 (healthy person, $\sim 1.0 \times 10^{-18}$ M). These results demonstrated that this method could be applied to the direct determination of miRNA-21 in serum samples without separation and enrichment. However, although patients can be discriminated from the healthy people, the type of disease cannot be clearly distinguished because of the complication with cancer that there are different subtypes of the same disease. It will be a huge challenge to design a gene biosensor for the diagnosis of disease types in future research.

To confirm the reliability of the method, a series of synthetic miRNA-21 at concentrations of 0, 10.0 aM, 0.1 fM, and 1.0 fM were spiked into healthy human blood serum (sample 2), respectively, to obtain the electrochemical signals. In Table S1, Supporting Information, the electrochemical response of miRNA-21 could reflect the real situation of the miRNA sample, indicating great potential for the miRNA analysis in clinical diagnosis.

## CONCLUSION

In summary, an ultrasensitive and highly specific electrochemical biosensor for miRNA assay was developed based on


DOI: 10.1021/am508690x
ACS Appl. Mater. Interfaces 2015, 7, 2979−2985

$Cd^{2+}$-modified TiP nanoparticles amplification and enhanced electron transfer using $Ru(NH_3)_6^{3+}$ as electronic wires. A proportional relationship was observed between the SWV peak currents and the logarithm of target miRNA-21 concentration in a linear range from 1.0 aM to 10.0 pM with a detection limit of 0.76 aM. At the same time, this proposed biosensor is sufficiently selective to discriminate the target miRNA from homologous miRNAs. Subsequently, the proposed strategy has successfully achieved the detection of human miRNAs from cancer patients' serum without separation and enrichment. Therefore, this biosensor is an attractive candidate for the development of an accurate, selective, and ultrasensitive method for miRNA expression profiling and clinical diagnostics.

## ■ ASSOCIATED CONTENT

### Supporting Information

TEM images of TiP−$Cd^{2+}$ nanoparticles modified with SA of different concentrations (Figure S1), polyacrylamide gel electrophoresis analysis of the RNA hybridization process (Figure S2), and reliability of the proposed method (Table S1). This material is available free of charge via the Internet at http://pubs.acs.org.

## ■ AUTHOR INFORMATION

### Corresponding Authors

*E-mail: jianglp@nju.edu.cn. Tel./Fax: +86-25-8359-7204.
*E-mail: jjzhu@nju.edu.cn. Tel./Fax: +86-25-8359-7204.

### Notes

The authors declare no competing financial interest.

## ■ ACKNOWLEDGMENTS

We greatly appreciate the support of the National Basic Research Program of China (2011CB933502) and the National Natural Science Foundation of China (21475057 and 21335004). This work is also supported by Program for New Century Excellent Talents in University (NCET-12-0256).

## ■ REFERENCES

(1) Bartel, D. P. MicroRNAs: Genomics, Biogenesis, Mechanism, and Function. *Cell* **2004**, *116*, 281−297.
(2) Volinia, S.; Calin, G. A.; Liu, C. G.; Ambs, S.; Cimmino, A.; Petrocca, F.; Visone, R.; Iorio, M.; Roldo, C.; Ferracin, M.; Prueitt, R. L.; Yanaihara, N.; Lanza, G.; Scarpa, A.; Vecchione, A.; Negrini, M.; Harris, C. C.; Croce, C. M. A MicroRNA Expression Signature of Human Solid Tumors Defines Cancer Gene Targets. *Proc. Natl. Acad. Sci. U.S.A.* **2006**, *103*, 2257−2261.
(3) Concepcion, C. P.; Bonetti, C.; Ventura, A. The MicroRNA-17-92 Family of MicroRNA Clusters in Development and Disease. *Cancer J.* **2012**, *18*, 262−267.
(4) Cissell, K. A.; Rahimi, Y.; Shrestha, S.; Hunt, E. A.; Deo, S. K. Bioluminescence-based Detection of MicroRNA, MiR21 in Breast Cancer Cells. *Anal. Chem.* **2008**, *80*, 2319−2325.
(5) Takada, S.; Berezikov, E.; Yamashita, Y.; Lagos-Quintana, M.; Kloosterman, W. P.; Enomoto, M.; Hatanaka, H.; Fujiwara, S.; Watanabe, H.; Soda, M.; Choi, Y. L.; Plasterk, R. H. A.; Cuppen, E.; Mano, H. Mouse MicroRNA Profiles Determined With a New and Sensitive Cloning Method. *Nucleic Acids Res.* **2006**, *34*, e115.
(6) Lee, R. C.; Ambros, V. An Extensive Class of Small RNAs in Caenorhabditis Elegans. *Science* **2001**, *294*, 862−864.
(7) Liu, C.-G.; Calin, G. A.; Meloon, B.; Gamliel, N.; Sevignani, C.; Ferracin, M.; Dumitru, C. D.; Shimizu, M.; Zupo, S.; Dono, M. An Oligonucleotide Microchip for Genome-Wide MicroRNA Profiling in Human and Mouse Tissues. *Proc. Natl. Acad. Sci. U.S.A.* **2004**, *101*, 9740−9744.
(8) Thomson, J. M.; Parker, J.; Perou, C. M.; Hammond, S. M. A Custom Microarray Platform for Analysis of MicroRNA Gene Expression. *Nat. Methods* **2004**, *1*, 47−53.
(9) Chen, C.; Ridzon, D. A.; Broomer, A. J.; Zhou, Z.; Lee, D. H.; Nguyen, J. T.; Barbisin, M.; Xu, N. L.; Mahuvakar, V. R.; Andersen, M. R.; Lao, K. Q.; Livak, K. J.; Guegler, K. J. Real-Time Quantification of MicroRNAs by Stem-Loop RT-PCR. *Nucleic Acids Res.* **2005**, *33*, e179.
(10) Hartig, J. S.; Grune, I.; Najafi-Shoushtari, S. H.; Famulok, M. Sequence-Specific Detection of MicroRNAs by Signal-Amplifying Ribozymes. *J. Am. Chem. Soc.* **2004**, *126*, 722−723.
(11) Wen, Y.; Xu, Y.; Mao, X.; Wei, Y.; Song, H.; Chen, N.; Huang, Q.; Fan, C.; Li, D. DNAzyme-Based Rolling-Circle Amplification DNA Machine for Ultrasensitive Analysis of MicroRNA in Drosophila Larva. *Anal. Chem.* **2012**, *84*, 7664−7669.
(12) Wang, X.-P.; Yin, B.-C.; Wang, P.; Ye, B.-C. Highly Sensitive Detection of MicroRNAs Based on Isothermal Exponential Amplification-Assisted Generation of Catalytic G-quadruplex DNAzyme. *Biosens. Bioelectron.* **2013**, *42*, 131−135.
(13) Zhang, Y.; Li, Z.; Cheng, Y.; Lv, X. Colorimetric Detection of MicroRNA and RNase H Activity in Homogeneous Solution with Cationic Polythiophene Derivative. *Chem. Commun.* **2009**, *22*, 3172−3174.
(14) Liu, Y.-Q.; Zhang, M.; Yin, B.-C.; Ye, B.-C. Attomolar Ultrasensitive MicroRNA Detection by DNA-Scaffolded Silver-Nanocluster Probe Based on Isothermal Amplification. *Anal. Chem.* **2012**, *84*, 5165−5169.
(15) Zhu, X.; Zhou, X.; Xing, D. Label-free Detection of MicroRNA: Two-step Signal Enhancement with a Hairpin-Probe-Based Graphene Fluorescence Switch and Isothermal Amplification. *Chem.—Eur. J.* **2013**, *19*, 5487−5494.
(16) Zhou, Y.; Wang, M.; Meng, X.; Yin, H.; Ai, S. Y. Amplified Electrochemical MicroRNA Biosensor Using a Hemin-G-quadruplex Complex as The Sensing Element. *RSC Adv.* **2012**, *2*, 7140−7145.
(17) Labib, M.; Khan, N.; Ghobadloo, S. M.; Cheng, J.; Pezacki, J. P.; Berezovski, M. V. Three-Mode Electrochemical Sensing of Ultralow MicroRNA Levels. *J. Am.. Chem. Soc.* **2013**, *135*, 3027−3038.
(18) Gao, Z.; Deng, H.; Shen, W.; Ren, Y. A Label-Free Biosensor for Electrochemical Detection of Femtomolar MicroRNAs. *Anal. Chem.* **2013**, *85*, 1624−1630.
(19) Fang, S.; Lee, H. J.; Wark, A. W.; Corn, R. M. Attomole Microarray Detection of MicroRNAs by Nanoparticle-Amplified SPR Imaging Measurements of Surface Polyadenylation Reactions. *J. Am. Chem. Soc.* **2006**, *128*, 14044−14046.
(20) Bi, S.; Zhang, J.; Hao, S.; Ding, C.; Zhang, S. S. Exponential Amplification for Chemiluminescence Resonance Energy Transfer Detection of MicroRNA in Real Samples Based on a Cross-Catalyst Strand-Displacement Network. *Anal. Chem.* **2011**, *83*, 3696−3702.
(21) Cheng, Y.; Lei, J. P.; Chen, Y. L.; Ju, H. X. Highly Selective Detection of MicroRNA Based on Distance-Dependent Electrochemiluminescence Resonance Energy Transfer Between CdTe Nanocrystals and Au Nanoclusters. *Biosens. Bioelectron.* **2014**, *51*, 431−436.
(22) Khan, N.; Cheng, J.; Pezacki, J. P.; Berezovski, M. V. Quantitative Analysis of MicroRNA in Blood Serum with Protein-Facilitated Affinity Capillary Electrophoresis. *Anal. Chem.* **2011**, *83*, 6196−6201.
(23) Abi, A.; Lin, M. H.; Pei, H.; Fan, C. H.; Ferapontova, E. E.; Zuo, X. L. Electrochemical Switching with 3D DNA Tetrahedral Nanostructures Self-Assembled at Gold Electrodes. *ACS Appl. Mater. Interfaces* **2014**, *6*, 8928−8931.
(24) Paleček, E.; Bartošík, M. Electrochemistry of Nucleic Acids. *Chem. Rev.* **2012**, *112*, 3427−3481.
(25) Lusi, E. A.; Passamano, M.; Guarascio, P.; Scarpa, A.; Schiavo, L. Innovative Electrochemical Approach for An Early Detection of MicroRNAs. *Anal. Chem.* **2009**, *81*, 2819−2822.
(26) Peng, Y.; Gao, Z. Amplified Detection of MicroRNA Based on Ruthenium Oxide Nanoparticle-Initiated Deposition of An Insulating Film. *Anal. Chem.* **2011**, *83*, 820−827.


DOI: 10.1021/am508690x
*ACS Appl. Mater. Interfaces* 2015, 7, 2979−2985

(27) Dong, H. F.; Jin, S.; Ju, H. X.; Hao, K.; Xu, L.-P.; Lu, H.; Zhang, X. J. Trace and Label-Free MicroRNA Detection Using Oligonucleotide Encapsulated Silver Nanoclusters as Probes. *Anal. Chem.* **2012**, *84*, 8670−8674.
(28) Pöhlmann, C.; Sprinzl, M. Electrochemical Detection of MicroRNAs via Gap Hybridization Assay. *Anal. Chem.* **2010**, *82*, 4434−4440.
(29) Wang, D.-C.; Hu, L.-H.; Zhou, Y.-H.; Huang, Y.-T.; Li, X.; Zhu, J.-J. Dual Channel Sensitive Detection of Hsa-miR-21 Based on Rolling Circle Amplification and Quantum Dots Tagging. *J. Biomed. Nanotechnol.* **2014**, *10*, 615−621.
(30) Cheng, Y. Q.; Zhang, X.; Li, Z. P.; Jiao, X. X.; Wang, Y. C.; Zhang, Y. L. Highly Sensitive Determination of MicroRNA Using Target-Primed and Branched Rolling-Circle Amplification. *Angew. Chem., Int. Ed.* **2009**, *48*, 3268−3272.
(31) Zhu, W. Y.; Su, X. P.; Gao, X. Y.; Dai, Z.; Zou, X. Y. A Label-Free and PCR-Free Electrochemical Assay for Multiplexed MicroRNA Profiles by Ligase Chain Reaction Coupling with Quantum Dots Barcodes. *Biosens. Bioelectron.* **2014**, *53*, 414−419.
(32) Meng, X. M.; Zhou, Y. L.; Liang, Q. J.; Qu, X. J.; Yang, Q. Q.; Yin, H. S.; Ai, S. Y. Electrochemical Determination of MicroRNA-21 Based on Biobarcode and Hemin/G-quadruplet DNAenzyme. *Analyst* **2013**, *138*, 3409−3415.
(33) Yin, H. S.; Zhou, Y. L.; Zhang, H. X.; Meng, X. M.; Ai, S. Y. Electrochemical Determination of MicroRNA-21 Based on graphene, LNA Integrated Molecular Beacon, AuNPs and Biotin Multifunctional Biobarcodes and Enzymatic Assay System. *Biosens. Bioelectron.* **2012**, *33*, 247−253.
(34) Wang, J. X.; Yi, X. Y.; Tang, H. L.; Han, H. X.; Wu, M. H.; Zhou, F. M. Direct Quantification of MicroRNA at Low Picomolar Level in Sera of Glioma Patients Using a Competitive Hybridization Followed by Amplified Voltammetric Detection. *Anal. Chem.* **2012**, *84*, 6400−6406.
(35) Asati, A.; Santra, S.; Kaittanis, C.; Nath, S.; Perez, J. M. Oxidase-Like Activity of Polymer-Coated Cerium Oxide Nanoparticles. *Angew. Chem., Int. Ed.* **2009**, *48*, 2308−2312.
(36) Gao, Z. Q.; Yang, Z. C. Detection of MicroRNAs Using Electrocatalytic Nanoparticle Tags. *Anal. Chem.* **2006**, *78*, 1470−1477.
(37) Wang, D. C.; Hu, L. H.; Zhou, H. M.; Abdel-Halim, E. S.; Zhu, J.-J. Molecular Beacon Structure Mediated Rolling Circle Amplification for Ultrasensitive Electrochemical Detection of MicroRNA Based on Quantum Dots Tagging. *Electrochem. Commun.* **2013**, *33*, 80−83.
(38) Feng, L.-N.; Bian, Z.-P.; Peng, J.; Jiang, F.; Yang, G.-H.; Zhu, Y.-D.; Yang, D.; Jiang, L.-P.; Zhu, J.-J. Ultrasensitive Multianalyte Electrochemical Immunoassay Based on Metal Ion Functionalized Titanium Phosphate Nanospheres. *Anal. Chem.* **2012**, *84*, 7810−7815.
(39) Wong, E. L. S.; Gooding, J. J. Charge Transfer through DNA: A Selective Electrochemical DNA Biosensor. *Anal. Chem.* **2006**, *78*, 2138−2144.
(40) Okahata, Y.; Kobayashi, T.; Tanaka, K.; Shimomura, M. Anisotropic Electric Conductivity in an Aligned DNA Cast Film. *J. Am. Chem. Soc.* **1998**, *120*, 6165−6166.
(41) Porath, D.; Bezryadin, A.; Vries, S. de; Dekker, C. Direct Measurement of Electrical Transport through DNA Molecules. *Nature* **2000**, *403*, 635−638.
(42) Heller, A. On the Hypothesis of Cathodic Protection of Genes. *Faraday Discuss.* **2000**, *116*, 1−13.
(43) Lewis, F. D.; Wu, T.; Zhang, Y.; Letsinger, R. L.; Greenfield, S. R.; Wasielewski, M. R. Distance-Dependent Electron Transfer in DNA Hairpins. *Science* **1997**, *277*, 673−676.
(44) Giese, B.; Amaudrut, J.; Köhler, A.-K.; Spormann, M.; Wessely, S. Direct Observation of Hole Transfer through DNA by Hopping between Adenine Bases and By Tunnelling. *Nature* **2001**, *412*, 318−320.
(45) Park, M. J.; Fujitsuka, M.; Kawai, K.; Majima, T. Direct Measurement of the Dynamics of Excess Electron Transfer Through Consecutive Thymine Sequence in DNA. *J. Am. Chem. Soc.* **2011**, *133*, 15320−15323.
(46) Abi, A.; Ferapontova, E. E. Unmediated by DNA Electron Transfer in Redox-Labeled DNA Duplexes End-Tethered to Gold Electrodes. *J. Am. Chem. Soc.* **2012**, *134*, 14499−14507.
(47) Feng, L.-N.; Peng, J.; Zhu, Y.-D.; Jiang, L.-P.; Zhu, J.-J. Synthesis of $Cd^{2+}$-functionalized Titanium Phosphate Nanoparticles and Application as Labels for Electrochemical Immunoassays. *Chem. Commun.* **2012**, *48*, 4474−4476.
(48) Hummers, W. S.; Offeman, R. E. Preparation of Graphitic Oxide. *J. Am. Chem. Soc.* **1958**, *80*, 1339−1339.
(49) Liu, J.; Lu, Y. Preparation of Aptamer-Linked Gold Nanoparticle Purple Aggregates for Colorimetric Sensing of Analytes. *Nat. Protoc.* **2006**, *1*, 246−252.
(50) Zheng, T. T.; Zhang, R.; Zhang, Q. F.; Tan, T. T.; Zhang, K.; Zhu, J.-J.; Wang, H. Ultrasensitive Dual-Channel Detection of Matrix Metalloproteinase-2 in Human Serum Using Gold-Quantum Dot Core−Satellite Nanoprobes. *Chem. Commun.* **2013**, *49*, 7881−7883.
(51) Shi, J.-J.; He, T.-T.; Jiang, F.; Abdel-Halim, E. S.; Zhu, J.-J. Ultrasensitive Multi-analyte Electrochemical Immunoassay Based on GNR-Modified Heated Screen-printed Carbon Electrodes and PS@PDA-Metal Labels for Rapid Detection of MMP-9 and IL-6. *Biosens. Bioelectron.* **2014**, *55*, 51−56.
(52) Tsujiura, M.; Ichikawa, D.; Komatsu, S.; Shiozaki, A.; Takeshita, H.; Kosuga, T.; Konishi, H.; Morimura, R.; Deguchi, K.; Fujiwara, H.; Okamoto, K.; Otsuji, E. Circulating MicroRNAs in Plasma of Patients with Gastric Cancers. *Br. J. Cancer* **2010**, *102* (7), 1174−1179.
(53) Jia, H. X.; Li, Z. P.; Liu, C. H.; Cheng, Y. Q. Ultrasensitive Detection of MicroRNAs by Exponential Isothermal Amplification. *Angew. Chem., Int. Ed.* **2010**, *49*, 5498−5501.
(54) Liu, L.; Xia, N.; Liu, H. P.; Kang, X. J.; Liu, X. S.; Xue, C.; He, X. L. Highly Sensitive and Label-Free Electrochemical Detection of MicroRNAs Based on Triple Signal Amplification of Multifunctional Gold Nanoparticles, Enzymes and Redox-Cycling Reaction. *Biosens. Bioelectron.* **2014**, *53*, 399−405.
(55) Hong, C. Y.; Chen, X.; Li, T.; Li, J.; Yang, H.-H.; Chen, J.-H.; Chen, G.-N. Ultrasensitive Electrochemical Detection of Cancer-Associated Circulating MicroRNA in Serum Samples Based on DNA Concatamers. *Biosens. Bioelectron.* **2013**, *50*, 132−136.
(56) Zhuang, J. Y.; Tang, D. P.; Lai, W. Q.; Chen, G.-N.; Yang, H. H. Immobilization-Free Programmable Hairpin Probe for Ultrasensitive Electronic Monitoring of Nucleic Acid Based on a Biphasic Reaction Mode. *Anal. Chem.* **2014**, *86*, 8400−8407.
(57) Zhang, X.; Wu, D. Z.; Liu, Z. J.; Cai, S. X.; Zhao, Y. P.; Chen, M.; Xia, Y. K.; Li, C. Y.; Zhang, J.; Chen, J. H. An Ultrasensitive Label-Free Electrochemical Biosensor for MicroRNA-21 Detection Based on a 2′-*O*-Methyl Modified DNAzyme and Duplex-Specific Nuclease Assisted Target Recycling. *Chem. Commun.* **2014**, *50*, 12375−12377.


DOI: 10.1021/am508690x
*ACS Appl. Mater. Interfaces* 2015, 7, 2979−2985